



Quantum state transfer by electromagnetic fields initialized in vacuum states in a system comprised of two consecutive cavities connected by an optical fiber in the presence of an external classical field

S. A. Hanoura¹ · M. M. A. Ahmed² · E. M. Khalil³ · A.-S. F. Obada²

Received: 26 April 2021 / Accepted: 6 December 2021 / Published online: 14 June 2022

© The Author(s), under exclusive licence to Springer Science+Business Media, LLC, part of Springer Nature 2022

Abstract

The Hamiltonian of a system of two successive Jaynes-Cummings cells (JCCs) indirectly coupled through an optical fiber mode under the influence of an external classical field (ECF) is simplified. In the framework of unitary transformations of the atomic and bosonic delocalized operators, the simplification is carried out. Three dispersive regimes, namely, large optical fiber coupling strength (OFCS), large detuning, and comparable OFCS and detuning are considered. The analytical solutions of Schrödinger equation for the different Hamiltonians when the fields are initially in the vacuum states and initially the first and the second atoms are in the excited and the ground states, respectively, are presented. The exploitation of the atomic population inversion function (APIF) of a single atom to the track of the quantum state transfer (QST) between the distant atoms is considered. The temporal evolution of the APIF is investigated. Effects of the external classical fields couplings (ECFCs), and the OFCS on the APIF are analyzed. Analysis of the resulted features based on the difference between the ECFC and the localized and delocalized atomic frequencies is presented. The collapses-revivals phenomenon (CRP) is clearer in absence of the ECF. The behavior of both the APIF and the CRP follow those for the overlap of evanescent fields model while the rates of the QST in the two schemes are un-equiv. The ECFs reformulate the initial quantum states and may augment the localized detuning. The ECFs either accelerate the transfer of the quantum state or delecterte it.

✉ S. A. Hanoura
sadek.ahmed10@yahoo.com

¹ Department of Basic Science, Faculty of Engineering, Sinai University, Al-Arish, Egypt

² Department of Mathematics, Faculty of Science, Al-Azhar University, Nasr City, Cairo 11884, Egypt

³ Department of Mathematics, College of Science, P.O. Box 11099, Taif University 21944, Taif, Saudi Arabia

Keywords External classical fields · Optical fiber mode · Effective Hamiltonians · Atomic population inversion · Collapses-revivals phenomenon

1 Introduction

Introducing the Jaynes–Cummings model (JCM) [1] was a key factor in understanding and realizing the interaction of matter and quantized electromagnetic field. JCM was designed for the study of the interaction of a two-level atom with a single mode quantized field. The JCM has received an enormous number of theoretical [1–3] and experimental [4, 5] studies. Such a studiousness attributes to its (*i.e.*, JCM) mathematical solubility and its richness in displaying many phenomena, such as Rabi oscillation [6–8], collapses-revivals phenomenon [2, 3, 9–20], the capability of producing non-classical fields [15, 17, 18, 20–25].

In the main time many researchers have turned their attentions and devoted the efforts towards the extensions and the generalizations of the JCM. As the JCM is considered as a standard model in addition to the alternative models, introduced by Dick [26] and Tavis and Cummings [27] in order to study the dynamics of N identical two-level atoms resonantly interacting with a single mode of the electromagnetic field. For instance, it has been extended and generalized to include multi-photon, multi-mode processes [28–40], multi-level systems [34–46], and the intensity-dependent JCM [19, 34–40, 44, 47] from theoretical point of view.

It is well known that the collapses-revivals phenomenon is a quite generic phenomenon for the quantum systems. Also, it represents one of the most important phenomena reported for the JCM since it manifests the granular nature of the initial state of the field and a good evidence of discreteness of photons [2, 48]. Experimental realizations of JCM were observed in optical and radio frequency domains [49, 50]. Theoretically, the CRP has been extensively studied in the framework of various aspects of quantum optics [38, 51–58]. The collapses-revivals behaviors in the investigation of the APIF represents the reversibility of the quantum states [2, 3, 59]. It was shown that, within the JCM, the collapses and revivals periods of the APIF either result in purely periodic behavior [60, 61] or display an irregular character [59] according to the form of the interaction.

In some physical models, the situation is confined to trapping the atoms in a cavity. Thus, the studies in the framework of cavity quantum electrodynamics (CQED) have been devoted especially to the efforts of addressing the problems of quantum networks and quantum states transfer (QST) in order to enhancing the quantum information distribution. The quantum networks is a process by which the transportation of quantum information between distant quantum systems can be accomplished. The QST is a measurement for the exchanged energy among the atomic systems in the form of photons across large distances. The QST plays a central role in the quantum information field due to its potential applications in many topics of the quantum mechanics, quantum cryptography, quantum computer, quantum purification, etc [62–74].

Recently, the researchers have studied the problem of remote cavities (completely isolated), across the network; they may be interacting and communicated [75–86].

In fact, the remote cavities are considered as generalizations of the JCM. Coupled-cavity arrays schemes "as generalization to the remote cavities" have attracted and received much attention. Such attention is due to the easy handling of the individual sites and the presence of relatively long-lived atomic states suitable for the purpose of encoding a quantum information. Controlling the dynamics of the system in a better way becomes easier with such systems due to their providing of a number of degrees of freedom where photons can be hopping from cavity to another. These cavities may be coupled through the overlap of evanescent cavity fields [87–90] and through an optical fiber [94, 95]. Connecting the distant cavities through an optical fiber is considered a fundamental setup for quantum networks [94, 95].

The purpose of the present article is to study the features and the phenomena of the APIF due to the influences of the ECF and the OFCS in an extension to Ref [96] and to assure that the entanglement dynamics in this model differs significantly from that for the [97] in addition to reviewing the difference between the rates of the QST.

The structure of the article is as follows: In Sect. 2, we introduce the Hamiltonian of the considered system and proceed towards its interaction picture to obtain the effective Hamiltonian for three approximate dispersive regime. In Sect. 3, we solve the Schrödinger equation for all introduced Hamiltonians giving analytical expressions for the final wavefunction. In Sect. 4, we employ the analytical results formulated in Sect. 3 to investigate the properties of the APIF. We devote Sect. 5 to discuss the influences of the relevant parameters on the evolution of the APIF. Finally, in Sect. 6, we present our conclusion depending on the analytic and the numerical results.

2 The Model

The considered model is a two coupled JCCs indirectly connected via an optical fiber. Each cavity contains a single two-level atom interact separately with a quantized electromagnetic field and driven by an ECF (see Fig. 1). The total Hamiltonian of the considered system can be cast as (we adopt $\hbar = 1$):

$$\hat{H} = \hat{H}_0 + \hat{H}_{int}. \quad (1)$$

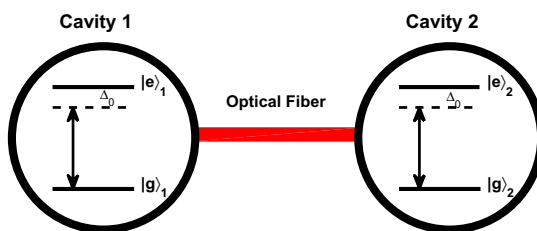


Fig. 1 Scheme of two distant standard JCM indirectly connected by an optical fiber. The atoms are driven by on resonance an ECF. The ket $|e\rangle_j$ ($|g\rangle_j$) represents the excited(lower) state of the j^{th} atom

Generally, the Hamiltonian \hat{H} can be written as follows:-

$$\hat{H} = \underbrace{\sum_{j=1}^2 \left[\omega_j \hat{a}_j^+ \hat{a}_j + \frac{\Omega_j}{2} \sigma_j^z + g_j (\hat{\sigma}_j^- + \hat{\sigma}_j^+) \right]}_{\hat{H}_0} + \omega_f \hat{b}^+ \hat{b} + \underbrace{v [b(\hat{a}_1^+ + \hat{a}_2^+) + H.C.] + i \sum_{j=1}^2 \lambda_j (\hat{a}_j + \hat{a}_j^+) (\hat{\sigma}_j^+ - \hat{\sigma}_j^-)}_{\hat{H}_{int}}, \tag{2}$$

The Hamiltonian \hat{H} , is a generalization of extensively studied earlier pictures [86, 98–103]. The parameters ω_j , ω_f , and Ω_j represent the frequencies of the quantized electromagnetic fields, the frequency of the fiber mode field and the frequencies of the atomic energies differences, respectively. Moreover, the parameters λ_j , g_j , and v stand for the atom-field coupling in the j^{th} cavity, the external classical field couplings (ECFCs), and the strength of the OFCS, respectively. The operators \hat{a}_j^+ , and \hat{a}_j are boson operators of the fields, they are controlled by the commutation relations $[\hat{a}_j, \hat{a}_k^+] = \hat{I} \delta_{jk}$: \hat{I} denotes the unity operator while δ refers to the Kronecker delta. The boson operators \hat{b}^+ , and \hat{b} describe the fiber operators and behave as \hat{a}_j^+ , and \hat{a}_j . The operators $\hat{\sigma}_j^-$, $\hat{\sigma}_j^+$, and σ_j^z are Pauli operators defined by $|g\rangle_j \langle e|$, $|e\rangle_j \langle g|$, and $|e\rangle_j \langle e| - |g\rangle_j \langle g|$, respectively.

2.1 Canonical transformations

The only motivation of the unitary canonical transformations is to obtain the wave-function of the quantum systems. Treatment of the present quantum system is not an easy task because of the presence of the rotating and counter-rotating terms, driving terms, and cavity-cavity coupling term. The elimination of the ECFs couplings and optical fiber mode coupling strengths and the counter-rotating parts is an essential requirement for the simplification of the Hamiltonian of the considered model. The elimination will be carried out through two common transformations [86, 98–103]. We shall review these canonical transformations in what follows:

2.1.1 The first transformation

The driven parts can be removed via the usage of the following canonical transformation

$$\begin{pmatrix} \sigma_j^z \\ \sigma_j^+ \\ \sigma_j^- \end{pmatrix} = \begin{pmatrix} \cos(2\eta_j) & -\sin(2\eta_j) & -\sin(2\eta_j) \\ \frac{1}{2} \sin(2\eta_j) & \cos^2(\eta_j) & -\sin^2(\eta_j) \\ \frac{1}{2} \sin(2\eta_j) & -\sin^2(\eta_j) & \cos^2(\eta_j) \end{pmatrix} \begin{pmatrix} S_j^z \\ S_j^+ \\ S_j^- \end{pmatrix}. \tag{3}$$

Which insures that $\hat{\sigma}_j^+ - \hat{\sigma}_j^- = S_j^+ - S_j^-$. The parameters η_j are chosen to be: $\eta_j = \frac{1}{2} \arccos(\frac{\Omega_j}{\sqrt{\Omega_j^2 + 4g_j^2}}) = \frac{1}{2} \arccos(\frac{\Omega_j}{\varphi_j})$. It is noted that the atomic frequency Ω_j is augmented to $\varphi_j = \sqrt{\Omega_j^2 + 4g_j^2}$ which includes the classical field couplings g_j . Also, when the rotating wave approximation is considered, the Hamiltonian of Eq.(1) can be written as follows:-

$$\hat{H} = \sum_{j=1}^2 [\omega_j \hat{a}_j^+ \hat{a}_j + \frac{\varphi_j}{2} S_j^z + i\lambda_j (\hat{a}_j \hat{S}_j^+ - \hat{a}_j^+ \hat{S}_j^-)] + \omega_f \hat{b}^+ \hat{b} + \nu (b(\hat{a}_1^+ + \hat{a}_2^+) + \hat{b}^+ (\hat{a}_1 + \hat{a}_2)). \tag{4}$$

The atomic new operators $\hat{S}_j^\pm = |\pm\rangle_j \langle \mp|_j$, and $\hat{S}_j^z = |+\rangle_j \langle +|_j - |-\rangle_j \langle -|_j$, where, the relations between the localized and localized atomic eigenstates are governed by

$$\begin{aligned} |+\rangle_j &= \cos \zeta_j |e\rangle_j + \sin \zeta_j |g\rangle_j, \\ |-\rangle_j &= \cos \zeta_j |g\rangle_j - \sin \zeta_j |e\rangle_j. \end{aligned} \tag{5}$$

2.1.2 The second transformation

The elimination of the converter part is executed via the exploitation of the following unitary canonical transformations $\hat{b} = \frac{\hat{C}_1 - \hat{C}_2}{\sqrt{2}}$, and $\hat{a}_j = \frac{1}{2}(\hat{C}_1 + \hat{C}_2 - (-)^j \sqrt{2} \hat{C}_0)$. Then, Eq. (4) will be on the form

$$\hat{H} = \sum_{\ell=0}^2 \tilde{\omega}_\ell \hat{C}_\ell^+ \hat{C}_\ell + \sum_{j=1}^2 \left[\frac{\varphi_j}{2} \hat{S}_j^z \right] + i \sum_{j=1}^2 \frac{\lambda_j}{2} [(\hat{C}_1 + \hat{C}_2 - (-)^j \sqrt{2} \hat{C}_0) \hat{S}_j^+ - H.C.], \tag{6}$$

For comprehensibility, we set $\omega_j = \omega_0 = \omega_f$ ($j = 1, 2$) which automatically leads to $\tilde{\omega}_\ell = \omega_0 - (-)^\ell \sqrt{2} \nu (1 - \delta_{0\ell})$.

2.2 Interaction picture

The interaction picture of the Hamiltonian depicted in Eq.(6) is controlled by $\hat{H}_I = e^{it\hat{H}_0} \hat{H}_{int} e^{-it\hat{H}_0}$, whereas

$$\hat{H} = \overbrace{\sum_{\ell=0}^2 \tilde{\omega}_\ell \hat{C}_\ell^+ \hat{C}_\ell + \sum_{j=1}^2 \left[\frac{\varphi_j}{2} \hat{S}_j^z \right]}^{\hat{H}_0} + i \overbrace{\sum_{j=1}^2 \frac{\lambda_j}{2} [(\hat{C}_1 + \hat{C}_2 - (-)^j \sqrt{2} \hat{C}_0) \hat{S}_j^+ - H.C.]}^{\hat{H}_{int}}. \tag{7}$$

By using the Baker–Campbell–Hausdorff formula [104], we have

$$\hat{H}_I = \hat{H}_{int} + (it)[\hat{H}_0, \hat{H}_{int}] + \frac{(it)^2}{2!} [\hat{H}_0, [\hat{H}_0, \hat{H}_{int}]] + \frac{(it)^3}{3!} [\hat{H}_0, [\hat{H}_0, [\hat{H}_0, \hat{H}_{int}]]] + \dots \tag{8}$$

Due to some commutation relations, one can cast the interaction picture of the Hamiltonian \hat{H}_I as follows:-

$$\hat{H}_I = \sum_{k=1}^2 \frac{i\lambda_k}{2} \left[\left(\sum_{j=1}^2 \hat{C}_j e^{-it(\hat{\omega}_j - \varphi_k)} + \sqrt{2}\hat{C}_0 e^{-it(\hat{\omega}_0 - \varphi_k)} \right) \hat{S}_k^+ - H.C. \right]. \quad (9)$$

2.3 The effective Hamiltonian

In this section we apply the method of Ref [105] to the current Hamiltonian in order to get the effective Hamiltonian in different dispersive regimes approximations. The effective Hamiltonian \hat{H}_{eff} can be written through the following relation [105], $\hat{H}_{eff} = \overline{\hat{H}_I(t)} + \frac{1}{2} \left([\overline{\hat{H}_I(t)}, \hat{V}_1(t)] - [\overline{\hat{H}_I(t)}, \hat{V}_1(t)] \right)$, the skew-Hermitian operator $\hat{V}_1(t)$ in its simplest form, is written as follows:-

$$\hat{V}_1(t) = \sum_{k=1}^2 \frac{i\lambda_k}{2} \left[\left(\sum_{j=1}^2 \frac{\hat{C}_j}{\hat{\omega}_j - \varphi_k} e^{-it(\hat{\omega}_j - \varphi_k)} + \sqrt{2} \frac{\hat{C}_0}{\omega_0 - \varphi_k} e^{-it(\omega_0 - \varphi_k)} \right) \hat{S}_k^+ + H.C. \right] \quad (10)$$

We are proceed to obtain the effective Hamiltonian in the language of the aforementioned limits *i.e.*, (i) large optical fiber mode coupling strength (ii) large detuning, and (iii) comparable optical fiber mode coupling strength and detuning. To make calculations more clearer and easier analytical computations, we again assume resonance of the atomic subsystems *i.e.*, $\Omega_j = \Omega$ besides symmetric couplings case *i.e.*, $\lambda_j = \lambda$, and $g_j = g \Rightarrow \varphi_j = \varphi$. Consequently, the detuning between the atomic modes \hat{S}_j , and \hat{C}_j are $\Delta_l = \varphi - \omega_l$, $l = 0, 1, 2$.

2.3.1 For large cavity-fiber coupling strength limit

This approximation is applicable when the condition $\sqrt{2}\nu \gg \Delta_0, \lambda$ is satisfied. Moreover, we assume that Δ_0, Δ_1 , and $\Delta_2 > \lambda$. These conditions ensure vanishing of the time average of both $\hat{V}_1(t)$ and $\hat{H}_I(t)$. The effective Hamiltonian is thus given

by the formula ($\mathfrak{S}_0 = \frac{\lambda^2}{4} \left[\sum_{j=1}^2 \frac{1}{\Delta_j} - \frac{2}{\Delta_0} \right]$)

$$\begin{aligned} \hat{H}_{eff}^{LC} = & \hat{H}_0 + \frac{\lambda^2}{4} \left[\sum_{j=1}^2 \frac{\hat{C}_j \hat{C}_j^+}{\Delta_j} + \frac{2\hat{C}_0 \hat{C}_0^+}{\Delta_0} \right] \sum_{j=1}^2 |+\rangle_j \langle +| \\ & - \frac{\lambda^2}{4} \left[\sum_{j=1}^2 \frac{\hat{C}_j^+ \hat{C}_j}{\Delta_j} + \frac{2\hat{C}_0^+ \hat{C}_0}{\Delta_0} \right] \sum_{j=1}^2 |-\rangle_j \langle -| + \mathfrak{S}_0 \sum_{\langle ij \rangle} \hat{S}_i^- \hat{S}_j^+. \end{aligned} \quad (11)$$

2.3.2 For large detuning limit

In this limit, the atom is highly detuned from the photonic modes: $\Delta_0 \gg \sqrt{2}\nu, \lambda$. Also, both $\hat{H}_I(t)$, and $\hat{V}_1(t)$ vanish. The effective Hamiltonian takes the following form:

$$\begin{aligned} \hat{H}_{eff}^{LD} = & \frac{\lambda^2}{8} \left[\left(\sqrt{2}\hat{C}_2\hat{C}_0^+ \left(\frac{1}{\Delta_0} + \frac{1}{\Delta_2} \right) + H.C. \right) \right. \\ & \left. + \left(\sqrt{2}\hat{C}_0\hat{C}_1^+ \left(\frac{1}{\Delta_0} + \frac{1}{\Delta_1} \right) + H.C. \right) \right] (\hat{S}_1^z - \hat{S}_2^z) \\ & + \frac{\lambda^2}{8} \left[\left(\hat{C}_1\hat{C}_2^+ \left(\frac{1}{\Delta_1} + \frac{1}{\Delta_2} \right) + H.C. \right) \right] (\hat{S}_1^z + \hat{S}_2^z) + \hat{H}_{eff}^{LC}. \end{aligned} \quad (12)$$

2.3.3 For comparable OFCS and detuning limit

This approximation requires that the frequency of one of the two atoms is nearby equal to that for the corresponding delocalized photonic modes. Such requirement can be written mathematically as $\Delta_1 \approx 0$. The effective Hamiltonian is reached and written as:

$$\begin{aligned} \hat{H}_{eff}^{CSD} = & \hat{H}_0 + \frac{i\lambda}{2} \left[\hat{C}_1(\hat{S}_1^+ + \hat{S}_2^+) - H.C. \right] + \frac{\lambda^2}{4} \left[\frac{\hat{C}_2\hat{C}_2^+}{\Delta_2} + \frac{2\hat{C}_0\hat{C}_0^+}{\Delta_0} \right] \sum_{j=1}^2 |+\rangle_j \langle +| \\ & - \frac{\lambda^2}{4} \left[\frac{\hat{C}_2^+\hat{C}_2}{\Delta_2} + \frac{2\hat{C}_0^+\hat{C}_0}{\Delta_0} \right] \sum_{j=1}^2 |-\rangle_j \langle -| + \frac{\lambda^2}{4} \left[\frac{1}{\Delta_2} - \frac{2}{\Delta_0} \right] \sum_{\langle i,j \rangle} \hat{S}_i^- \hat{S}_j^+. \end{aligned} \quad (13)$$

Now, we proceed to calculate the time-dependent wavefunction of the mentioned different Hamiltonians.

3 The wavefunction

We consider the two modes and the fiber mode to be initially prepared in the vacuum states, and the first atom is in its excited state while the second atom is in ground state. Eventually, according to the delocalized modes, the initial wavefunction becomes of the form

$$|\Psi_{AF}(0)\rangle = A_1(0)|+ +000\rangle + A_2(0)|+ -000\rangle + A_3(0)|- +000\rangle + A_4(0)|- -000\rangle. \quad (14)$$

Based on the Hamiltonian (6) and the considered wavefunction (14) the time dependent wavefunction of the considered system can be formed as follows $[A_j(0) = \sin \eta \cos \eta \delta_{1j} + \cos^2 \eta \delta_{2j} - \sin^2 \eta \delta_{3j} - \sin \eta \cos \eta \delta_{4j}]$:

$$|\Psi_{AF}(t)\rangle = \sum_{j=1}^{19} A_j(t)|\psi_j\rangle. \tag{15}$$

The wavefunction is assumed initially normalized and according to Schrödinger’s equation, it stays normalized as it evolves in time *i.e.*, $\sum_{j=1}^{19} |A_j(t)|^2 = 1$. Within the delocalized bosonic modes, it is formed as follows:

$$|\Psi_{AF}(t)\rangle = \sum_{j=1}^{19} \mathfrak{B}_j(t)|\psi_j\rangle. \tag{16}$$

with

$$\begin{pmatrix} \mathfrak{B}_k \\ \mathfrak{B}_5 \\ \mathfrak{B}_6 \\ \mathfrak{B}_7 \\ \mathfrak{B}_8 \\ \mathfrak{B}_9 \\ \mathfrak{B}_{10} \\ \mathfrak{B}_{11} \\ \mathfrak{B}_{12} \\ \mathfrak{B}_{13} \\ \mathfrak{B}_{14} \\ \mathfrak{B}_{15} \\ \mathfrak{B}_{16} \\ \mathfrak{B}_{17} \\ \mathfrak{B}_{18} \\ \mathfrak{B}_{19} \end{pmatrix} = \begin{pmatrix} A_k, \quad k = 1, \dots, 4 \\ \left(\frac{A_5}{2} + \frac{A_6}{2} + \frac{A_7}{\sqrt{2}}\right) \\ \left(\frac{A_5}{2} + \frac{A_6}{2} - \frac{A_7}{\sqrt{2}}\right) \\ \frac{1}{\sqrt{2}}(A_5 - A_6) \\ \left(\frac{A_8}{2} + \frac{A_9}{2} + \frac{A_{10}}{\sqrt{2}}\right) \\ \left(\frac{A_8}{2} + \frac{A_9}{2} - \frac{A_{10}}{\sqrt{2}}\right) \\ \frac{1}{\sqrt{2}}(A_8 - A_9) \\ \left(\frac{A_{11}}{2} + \frac{A_{12}}{2} + \frac{A_{13}}{\sqrt{2}}\right) \\ \left(\frac{A_{11}}{2} + \frac{A_{12}}{2} - \frac{A_{13}}{\sqrt{2}}\right) \\ \frac{1}{\sqrt{2}}(A_{11} - A_{12}) \\ \left(\frac{A_{17}}{2\sqrt{2}} + \frac{A_{14}}{2} + \frac{A_{18}}{2\sqrt{2}} - \frac{A_{19}}{\sqrt{2}}\right) \\ \left(\frac{A_{15}}{2} - \frac{A_{16}}{2} + \frac{A_{17}}{2} - \frac{A_{18}}{2}\right) \\ \left(-\frac{A_{15}}{2} + \frac{A_{16}}{2} + \frac{A_{17}}{2} - \frac{A_{18}}{2}\right) \\ \left(\frac{\sqrt{2}A_{14}}{4} + \frac{A_{15}}{2} + \frac{A_{16}}{2} + \frac{A_{17}}{4} + \frac{A_{18}}{4} + \frac{A_{19}}{2}\right) \\ \left(\frac{\sqrt{2}A_{14}}{4} - \frac{A_{15}}{2} - \frac{A_{16}}{2} + \frac{A_{17}}{4} + \frac{A_{18}}{4} + \frac{A_{19}}{2}\right) \\ \left(\frac{-\sqrt{2}A_{14}}{2} + \frac{A_{17}}{2} + \frac{A_{18}}{2}\right) \end{pmatrix}, \text{ while } \begin{pmatrix} |\psi_1\rangle \\ |\psi_2\rangle \\ |\psi_3\rangle \\ |\psi_4\rangle \\ |\psi_5\rangle \\ |\psi_6\rangle \\ |\psi_7\rangle \\ |\psi_8\rangle \\ |\psi_9\rangle \\ |\psi_{10}\rangle \\ |\psi_{11}\rangle \\ |\psi_{12}\rangle \\ |\psi_{13}\rangle \\ |\psi_{14}\rangle \\ |\psi_{15}\rangle \\ |\psi_{16}\rangle \\ |\psi_{17}\rangle \\ |\psi_{18}\rangle \\ |\psi_{19}\rangle \end{pmatrix} = \begin{pmatrix} | + + 0 0 0 \rangle \\ | + - 0 0 0 \rangle \\ | - + 0 0 0 \rangle \\ | - - 0 0 0 \rangle \\ | + - 1 0 0 \rangle \\ | + - 0 1 0 \rangle \\ | + - 0 0 1 \rangle \\ | - + 1 0 0 \rangle \\ | - + 0 1 0 \rangle \\ | - + 0 0 1 \rangle \\ | - - 1 0 0 \rangle \\ | - - 0 1 0 \rangle \\ | - - 0 0 1 \rangle \\ | - - 1 1 0 \rangle \\ | - - 0 1 1 \rangle \\ | - - 1 0 1 \rangle \\ | - - 2 0 0 \rangle \\ | - - 0 2 0 \rangle \\ | - - 0 0 2 \rangle \end{pmatrix}. \tag{17}$$

While the atomic density matrix for the two atoms, in the basis of $|++\rangle, |+-\rangle, |-+\rangle,$ and $|--\rangle,$ is

$$\rho^{(12)}(t) = \begin{pmatrix} |\mathbb{B}_1(t)|^2 & \mathbb{B}_1(t)\mathbb{B}_2^*(t) & \mathbb{B}_1(t)\mathbb{B}_3^*(t) & \mathbb{B}_1(t)\mathbb{B}_4^*(t) \\ \mathbb{B}_2(t)\mathbb{B}_1^*(t) & |\mathbb{B}_2(t)|^2 + \sum_{j=5}^7 |\mathbb{B}_j(t)|^2 & \mathbb{B}_2(t)\mathbb{B}_3^*(t) + \sum_{j=5}^7 \mathbb{B}_j(t)\mathbb{B}_{j+3}^*(t) & \mathbb{B}_2(t)\mathbb{B}_4^*(t) + \sum_{j=5}^7 \mathbb{B}_j(t)\mathbb{B}_{j+6}^*(t) \\ \mathbb{B}_3(t)\mathbb{B}_1^*(t) & \mathbb{B}_3(t)\mathbb{B}_2^*(t) + \sum_{j=5}^7 \mathbb{B}_{j+3}(t)\mathbb{B}_j^*(t) & |\mathbb{B}_3(t)|^2 + \sum_{j=8}^{10} |\mathbb{B}_j(t)|^2 & \mathbb{B}_3(t)\mathbb{B}_4^*(t) + \sum_{j=8}^{10} \mathbb{B}_j(t)\mathbb{B}_{j+3}^*(t) \\ \mathbb{B}_4(t)\mathbb{B}_1^*(t) & \mathbb{B}_4(t)\mathbb{B}_2^*(t) + \sum_{j=5}^7 \mathbb{B}_{j+6}(t)\mathbb{B}_j^*(t) & \mathbb{B}_4(t)\mathbb{B}_3^*(t) + \sum_{j=8}^{10} \mathbb{B}_{j+3}(t)\mathbb{B}_j^*(t) & |\mathbb{B}_4(t)|^2 + \sum_{j=11}^{19} |\mathbb{B}_j(t)|^2 \end{pmatrix}. \tag{18}$$

Then, the atomic density matrix for 1^{st} -atom, in the basis of $|+\rangle_1,$ and $|-\rangle_1,$ is

$$\rho^{[1]}(t) = \begin{pmatrix} \sum_{j=1}^2 |\mathbb{B}_j(t)|^2 + \sum_{j=5}^7 |\mathbb{B}_j(t)|^2 & \sum_{j=1}^2 \mathbb{B}_j(t)\mathbb{B}_{j+2}^*(t) + \sum_{j=5}^7 \mathbb{B}_j(t)\mathbb{B}_{j+6}^*(t) \\ \sum_{j=1}^2 \mathbb{B}_{j+2}(t)\mathbb{B}_j^*(t) + \sum_{j=5}^7 \mathbb{B}_{j+6}(t)\mathbb{B}_j^*(t) & \sum_{j=3}^4 |\mathbb{B}_j(t)|^2 + \sum_{j=8}^{19} |\mathbb{B}_j(t)|^2 \end{pmatrix} \tag{19}$$

Then, the atomic density matrix for 2^{nd} -atom, in the basis of $|+\rangle_2,$ and $|-\rangle_2,$ is

$$\rho^{[2]}(t) = \begin{pmatrix} |\mathbb{B}_1(t)|^2 + |\mathbb{B}_3(t)|^2 + \sum_{j=8}^{10} |\mathbb{B}_j(t)|^2 & \sum_{j=1,3} \mathbb{B}_j(t)\mathbb{B}_{j+1}^*(t) + \sum_{j=8}^{10} \mathbb{B}_j(t)\mathbb{B}_{j+3}^*(t) \\ \sum_{j=1,3} \mathbb{B}_{j+1}(t)\mathbb{B}_j^*(t) + \sum_{j=8}^{10} \mathbb{B}_{j+3}(t)\mathbb{B}_j^*(t) & |\mathbb{B}_2(t)|^2 + \sum_{j=4}^7 |\mathbb{B}_j(t)|^2 + \sum_{j=11}^{19} |\mathbb{B}_j(t)|^2 \end{pmatrix} \tag{20}$$

The three roots of the cubic equation $\tau^3 + X_1\tau^2 + X_2\tau + X_3 = 0,$ can be cast as follows:-

$$\begin{aligned} \tau_j &= -\frac{X_1}{3} + \frac{2}{3} \left(\sqrt{X_1^2 - 3X_2} \right) \cos(\theta_j), \quad j = \mathbf{1,2,3} \\ \theta_j &= \left(\frac{1}{3} \cos^{-1} \left[\frac{9X_1X_2 - 2X_1^3 - 27X_3}{2(X_1^2 - 3X_2)^{\frac{3}{2}}} \right] + (j-1) \frac{2\pi}{3} \right). \end{aligned} \tag{21}$$

3.1 For the full Hamiltonian

Because of the rather complicated calculations of the solution of the Schrödinger equations of the considered system, we only content with displaying analytical expressions for the coefficients of the wavefunction of the full Hamiltonian depicted in Eq.(6).

$$\begin{pmatrix} A_1(t) \\ A_2(t) \\ A_3(t) \\ A_4(t) \\ A_{11}(t) \\ A_{12}(t) \\ A_{13}(t) \end{pmatrix} = \begin{pmatrix} e^{-it\varphi} \sum_{j=1}^{10} K_j e^{itn_j} \\ \frac{1}{2} \left(e^{it \frac{\Delta_0}{2}} \left[c_0 \cos \left(t \sqrt{\left(\frac{\Delta_0}{2} \right)^2 + \lambda^2} \right) + d_0 \sin \left(t \sqrt{\left(\frac{\Delta_0}{2} \right)^2 + \lambda^2} \right) \right] + \sum_{j=1}^3 M_j^{[3]} e^{it\tau_j^{[3]}} \right) \\ -\frac{1}{2} \left(e^{it \frac{\Delta_0}{2}} \left[c_0 \cos \left(t \sqrt{\left(\frac{\Delta_0}{2} \right)^2 + \lambda^2} \right) + d_0 \sin \left(t \sqrt{\left(\frac{\Delta_0}{2} \right)^2 + \lambda^2} \right) \right] + \sum_{j=1}^3 M_j^{[3]} e^{it\tau_j^{[3]}} \right) \\ A_4(0)e^{-it\varphi} \\ \sum_{j=1}^3 M_j^{[1]} e^{it(\tau_j^{[1]} + \Delta_1)} \\ \sum_{j=1}^3 M_j^{[2]} e^{it(\tau_j^{[2]} + \Delta_2)} \\ e^{it \frac{\Delta_0}{2}} \left(\kappa_0 \cos \left(t \sqrt{\left(\frac{\Delta_0}{2} \right)^2 + \lambda^2} \right) + \kappa_1 \sin \left(t \sqrt{\left(\frac{\Delta_0}{2} \right)^2 + \lambda^2} \right) \right) \end{pmatrix}, \tag{22}$$

with $[\kappa_0, \kappa_1, c_0, d_0] = [0, \frac{-\frac{\lambda}{2}(A_2(0) - A_3(0))}{\sqrt{\left(\frac{\Delta_0}{2}\right)^2 + \lambda^2}}, A_2(0) - A_3(0), \frac{-i \frac{\Delta_0}{2}(A_2(0) - A_3(0))}{\sqrt{\left(\frac{\Delta_0}{2}\right)^2 + \lambda^2}}]$. Moreover, the $X_1, X_2,$ and X_3 for the coefficients $A_j(t)$ ($j = 2, 3, 11, 12$) are as follows:-

	$A_{11}(t)$	$A_{12}(t)$	$A_{2,3}(t)$
X_1	$2\Delta_1 - \Delta_2$	$2\Delta_2 - \Delta_1$	$-(\Delta_1 + \Delta_2)$
X_2	$-(\lambda^2 + \Delta_1\Delta_2 - \Delta_1^2)$	$-(\lambda^2 + \Delta_2\Delta_1 - \Delta_2^2)$	$-(\lambda^2 - \Delta_1\Delta_2)$
X_3	$\frac{\lambda^2}{2}(\Delta_2 - \Delta_1)$	$\frac{\lambda^2}{2}(\Delta_1 - \Delta_2)$	$\frac{\lambda^2}{2}(\Delta_1 + \Delta_2)$

(23)

Furthermore, the coefficients $M_1^{[j]}, M_2^{[j]},$ and $M_3^{[j]}$, in the language of the matrices, can be read as follows:-

$$\begin{pmatrix} M_1^{[j]} \\ M_2^{[j]} \\ M_3^{[j]} \end{pmatrix} = \begin{pmatrix} 1 & 1 & 1 \\ \varphi_1^{[j]} i & \varphi_2^{[j]} i & \varphi_3^{[j]} i \\ -\varphi_1^{[j]} & -\varphi_2^{[j]} & -\varphi_3^{[j]} \end{pmatrix}^{-1} \begin{pmatrix} \Re_0 \\ \Re_1 \\ \Re_2 \end{pmatrix}. \tag{24}$$

Also, the parameters $\Re_0, \Re_1,$ and $\Re_2,$ for different j can be arranged as follows:-

	\Re_0	\Re_1	\Re_2
$j = 1$	0	0	$\cos 2\eta$
$j = 2$	$-0.5 \cos 2\eta$	$-0.5 \cos 2\eta$	0
$j = 3$	$0.5 i \lambda \Delta_1 \cos 2\eta$	$0.5 i \lambda \Delta_2 \cos 2\eta$	$-\lambda^2 \cos 2\eta$

(25)

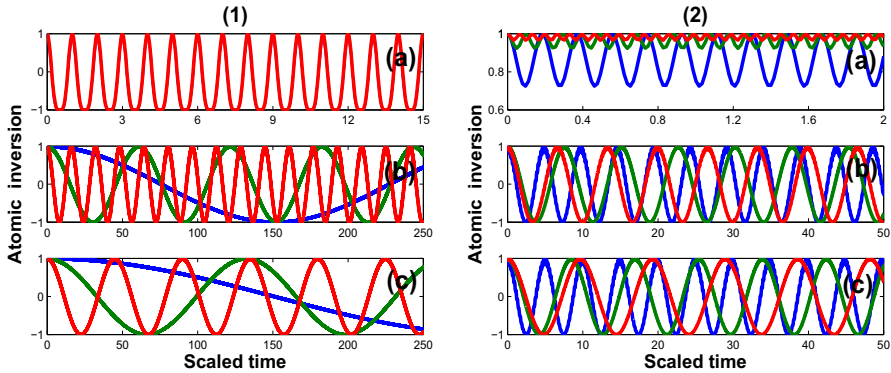


Fig. 2 The time evolution of the 1^{st} -atom, $W_1(t)$, for the Hamiltonian Eq.(1) subject to the state Eq.(14) while the system parameters values are $\omega_0 = 10\lambda$, $\eta = 0$ and in (a) $\nu_0 = 0\lambda$, (b) $\nu_0 = 20\lambda$, and (c) $\nu_0 = 25\lambda$, with the blue curve $\vartheta_0 = 5$, the green curve $\vartheta_0 = 10$, and the red curve $\vartheta_0 = 15$ where in (1) $\Delta_0 = \nu_0$, and $\nu = \frac{\vartheta_0}{\sqrt{2}}$, and in (2) $\nu = \frac{\nu_0}{\sqrt{2}}$, and $\Delta_0 = \vartheta_0$

More, the parameters n_j are the eigenvalues of the 10^{th} degree algebraic equation which is formed as follows:-

$$\sum_{l=0}^{10} n^{10-l} X_l = 0. \tag{26}$$

This algebraic equation is the characteristic of the ODE of $\tilde{B}_1(t)$ which is formulated as follows:-

$$\left[\aleph_{11} \left(\frac{d}{dt} - 2i \Delta_1 \right) \aleph_0 \left(\frac{d}{dt} \right) - \aleph_1 \left(\frac{d}{dt} - 2i \Delta_1 \right) \aleph_{00} \left(\frac{d}{dt} \right) \right] \tilde{B}_1(t) = 0. \tag{27}$$

The differentiable operators \aleph_{00} , and \aleph_{11} are not shown here. The parameters K_j can be determined in an easily manner was previously used in [106]. The analytical expressions of the remainder coefficients can easily be derived. In what follows we consider the cases of the different regimes.

3.2 For large OFCS and large detuning

For the Hamiltonians in Eqs.(11, 12), the nonzero coefficients of the final wavefunction are written as follows:-

$$\begin{pmatrix} A_1(t) \\ A_2(t) \\ A_3(t) \\ A_4(t) \end{pmatrix} = \begin{pmatrix} A_1(0) \exp \left(-it \left(\varphi + \frac{\lambda^2}{2} \left(\frac{1}{\Delta_1} + \frac{1}{\Delta_2} + \frac{2}{\Delta_0} \right) \right) \right) \\ e^{-it \frac{\lambda^2}{4} \left(\frac{1}{\Delta_1} + \frac{1}{\Delta_2} + \frac{2}{\Delta_0} \right)} \left[A_2(0) \cos \left(\frac{t \lambda^2}{4} \left(\frac{1}{\Delta_1} + \frac{1}{\Delta_2} - \frac{2}{\Delta_0} \right) \right) - i A_3(0) \sin \left(\frac{t \lambda^2}{4} \left(\frac{1}{\Delta_1} + \frac{1}{\Delta_2} - \frac{2}{\Delta_0} \right) \right) \right] \\ e^{-it \frac{\lambda^2}{4} \left(\frac{1}{\Delta_1} + \frac{1}{\Delta_2} + \frac{2}{\Delta_0} \right)} \left[A_3(0) \cos \left(\frac{t \lambda^2}{4} \left(\frac{1}{\Delta_1} + \frac{1}{\Delta_2} - \frac{2}{\Delta_0} \right) \right) - i A_2(0) \sin \left(\frac{t \lambda^2}{4} \left(\frac{1}{\Delta_1} + \frac{1}{\Delta_2} - \frac{2}{\Delta_0} \right) \right) \right] \\ A_4(0) \exp(it\varphi) \end{pmatrix}. \tag{28}$$

3.3 For comparable OFCS and detuning

For the Hamiltonian in Eq.(13), the nonzero coefficients of the final wavefunction can be written as follows:-

$$\begin{pmatrix} A_1(t) \\ A_2(t) \\ A_3(t) \\ A_5(t) \\ A_8(t) \\ A_{11}(t) \\ A_{17}(t) \end{pmatrix} = \begin{pmatrix} \sum_{j=1}^3 K_j \exp\left(it\left(k_j - \varphi - \frac{\lambda^2}{2}\left(\frac{1}{\Delta_2} + \frac{2}{\Delta_0}\right)\right)\right) \\ \frac{1}{4} e^{-it\frac{\lambda^2}{2}\left(\frac{1}{\Delta_2} + \frac{2}{\Delta_0}\right)} \left(+D_{23}(0)e^{it\frac{\lambda^2}{4}\left(\frac{1}{\Delta_2} - \frac{2}{\Delta_0}\right)} + e^{0.5it(\Delta_1 + \frac{\lambda^2}{\Delta_0})} [e_1 \cos(t\Xi) + e_2 \sin(t\Xi)] \right) \\ \frac{1}{4} e^{-it\frac{\lambda^2}{2}\left(\frac{1}{\Delta_2} + \frac{2}{\Delta_0}\right)} \left(-D_{23}(0)e^{it\frac{\lambda^2}{4}\left(\frac{1}{\Delta_2} - \frac{2}{\Delta_0}\right)} + e^{0.5it(\Delta_1 + \frac{\lambda^2}{\Delta_0})} [e_1 \cos(t\Xi) + e_2 \sin(t\Xi)] \right) \\ \frac{1}{2} \sum_{j=1}^3 M_j \exp\left(it\left(m_j - \omega_2 - \frac{\lambda^2}{4}\left(\frac{1}{\Delta_2} + \frac{2}{\Delta_0}\right)\right)\right) \\ \frac{1}{2} \sum_{j=1}^3 M_j \exp\left(it\left(m_j - \omega_2 - \frac{\lambda^2}{4}\left(\frac{1}{\Delta_2} + \frac{2}{\Delta_0}\right)\right)\right) \\ e^{0.5it(\Delta_1 - \frac{\lambda^2}{2\Delta_2})} [e_{11} \cos(t\Xi) + e_{22} \sin(t\Xi)] \\ \sum_{j=1}^3 L_j \exp\left(it\left(l_j - 2\omega_2 + \varphi\right)\right) \end{pmatrix}, \tag{29}$$

Based on the imposed constraints in the current work, one via minor algebra operations, one can conclude that $[\Re_{23} = A_2(0) + A_3(0), [e_1, e_2, e_{11}, e_{22}, \Xi] = [\Re_{23}, -0.5i\Xi^{-1}(\Delta_1 + \frac{\lambda^2}{2\Delta_2})\Re_{23}, 0, -0.5\lambda\Xi^{-1}\Re_{23}, 0.5\sqrt{\Delta_1^2 + \frac{\lambda^4}{4\Delta_2^2} + \frac{\Delta_1\lambda^2}{\Delta_2} + 2\lambda^2}]$. Moreover, the parameters $k_j, l_j,$ and m_j all are copy of τ_j shown in (21). Moreover, the $X_1, X_2,$ and X_3 for the coefficients $A_j(t)$ ($j = 1, 17, 5, 8$) are as follows $[s = \Delta_1 + \frac{\lambda^2}{4}\left(\frac{1}{\Delta_2} + \frac{2}{\Delta_0}\right)]$:-

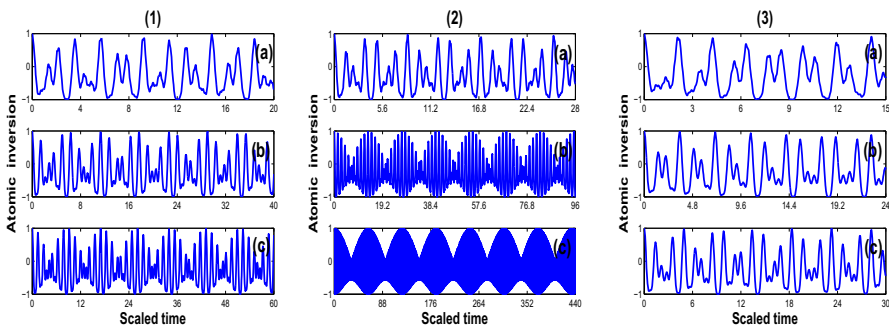


Fig. 3 The time evolution of the APIF of the 1st-atom, $W_1(t)$, for the Hamiltonian Eq.(1) subject to the state Eq.(14) while the system parameters values are $\omega_0 = 10\lambda, \eta = 0$ and in (a) $\Delta_0 = 5\lambda,$ (b) $\Delta_0 = 10\lambda,$ and (c) $\Delta_0 = 15\lambda,$ while in (1) $\Delta_1 = 0,$ (2) $\Delta_1 = -0.1\lambda,$ and (3) $\Delta_1 = 0.1\lambda$

	$A_{17}(t)$	$A_{5,8}(t)$
X_1	$-\left(3s - \frac{\lambda^2}{4} \left(\frac{1}{\Delta_2} - \frac{2}{\Delta_0}\right)\right)$	$\frac{\lambda^2}{4} \left(\frac{1}{\Delta_2} - \frac{2}{\Delta_0}\right)$
X_2	$-\left(\frac{3\lambda^2}{2} - 2s \left(s - \frac{\lambda^2}{4} \left(\frac{1}{\Delta_2} - \frac{2}{\Delta_0}\right)\right)\right)$	$-\left(s^2 + \frac{3\lambda^2}{2}\right)$
X_3	$\lambda^2 s$	$-2\lambda^2 s$

(30)

The coefficients $\mathcal{V}_j \equiv K_j, M_j,$ and L_j are controlled by $(\mathbf{v}_j \equiv k_j, l_j,$ and $m_j)$:-

$$\begin{pmatrix} \mathcal{V}_1 \\ \mathcal{V}_2 \\ \mathcal{V}_3 \end{pmatrix} = \begin{pmatrix} 1 & 1 & 1 \\ \mathbf{v}_1 i & \mathbf{v}_2 i & \mathbf{v}_3 i \\ -\mathbf{v}_1^2 & -\mathbf{v}_2^2 & -\mathbf{v}_3^2 \end{pmatrix}^{-1} \begin{pmatrix} \Re_{00} \\ \Re_{11} \\ \Re_{22} \end{pmatrix}. \tag{31}$$

	$K_j(t)$	$M_j(t)$	$L_j(t)$
\Re_{00}	0	0	0
\Re_{11}	0	0	$-\lambda \sin(\eta) \cos(\eta)$
\Re_{22}	$-0.5\lambda^2 \sin(\eta) \cos(\eta)$	$\frac{\lambda^2}{\sqrt{2}} \sin(\eta) \cos(\eta)$	$i\lambda \left(s + \frac{\lambda^2}{4} \left(\frac{1}{\Delta_2} - \frac{2}{\Delta_0}\right)\right) \sin(\eta) \cos(\eta)$

(32)

Due to the enumerated relations-above, one is in a position to discuss many quantum aspects. But here we content to review the CRP in to the atomic inversion of a single atom.

4 Collapses-revivals phenomenon (CRP)

The CRP represents one of the most important nonclassical phenomena in the field of quantum optics. The observation of this phenomenon occurred during the course of interaction between the field and the atom within a cavity. This phenomenon is a pure quantum mechanical effect and having its origin in the granular structure of the photon-number distribution of the initial field [107]. The CRP has been seen in nonlinear optics

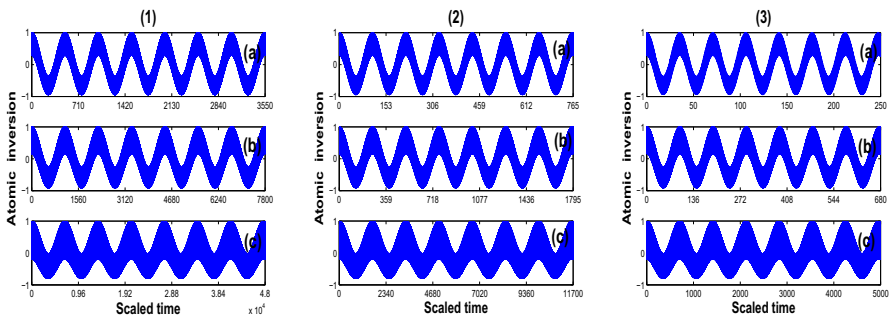


Fig. 4 The time evolution of the APIF of the 1^{st} -atom, $W_1(t)$, for the Hamiltonian Eq.(1) subject to the state Eq.(14) while the system parameters values are $\omega_0 = \Omega = 100\lambda$, and in (a) $\eta = \frac{0.900\pi}{9}$, (b) $\eta = \frac{1.000\pi}{9}$, and (c) $\eta = \frac{1.250\pi}{9}$, while in (1) $\sqrt{2}\nu = 5\lambda$, (2) $\sqrt{2}\nu = 10\lambda$, and in (3) $\sqrt{2}\nu = 15\lambda$

for the single-mode mean-photon number of the Kerr nonlinear coupler [108] when the modes are initially prepared in coherent light, however, in this case the origin of the occurrence of such a phenomenon is in the presence of nonlinearity in the system (third-order nonlinearity specified by the cubic susceptibility). Also, the atomic density operator elements for a one atom in the old basis have the forms

$$\begin{aligned}
 \rho_{ee}^{[i]} &= \rho_{++}^{[i]} \cos^2 \eta - (\rho_{+-}^{[i]} + \rho_{-+}^{[i]}) \sin \eta \cos \eta - \rho_{--}^{[i]} \sin^2 \eta, \\
 \rho_{eg}^{[i]} &= \rho_{+-}^{[i]} \cos^2 \eta + (\rho_{++}^{[i]} - \rho_{--}^{[i]}) \sin \eta \cos \eta - \rho_{-+}^{[i]} \sin^2 \eta, \\
 \rho_{ge}^{[i]} &= \rho_{-+}^{[i]} \cos^2 \eta + (\rho_{++}^{[i]} - \rho_{--}^{[i]}) \sin \eta \cos \eta - \rho_{+-}^{[i]} \sin^2 \eta, \\
 \rho_{gg}^{[i]} &= \rho_{++}^{[i]} \sin^2 \eta + (\rho_{+-}^{[i]} + \rho_{-+}^{[i]}) \sin \eta \cos \eta - \rho_{--}^{[i]} \cos^2 \eta.
 \end{aligned} \tag{33}$$

The APIF, $W(t)$, which represents the difference between the population of the excited and the ground states. *Approval of the APIF for the study of the QST is attributed to the easiness of the determination of both the places of the perfect QST (PQST) and the places of the synchronization of the two atoms (STAs): for specific times, the PQST is possible when $\sum_{i=1}^2 W_i(t_s) = 0$ while the STAs is possible if $\sum_{i=1}^2 (-)^{i+1} W_i(t_v) = 0$ ($W_1(t)$ is for the 1st atom while $W_2(t)$ is for the 2nd atom). The APIF can be formulated as follows:-*

$$W_i(t) = \cos(2\eta)(\rho_{++}^{[i]} - \rho_{--}^{[i]}) - \sin(2\eta)(\rho_{+-}^{[i]} + \rho_{-+}^{[i]}). \tag{34}$$

5 Numerical results and discussion

In the present section, our interest focuses on the investigation of the APIF in accordance with different dispersive regimes. We give comments on the resulted features due to the variation of the inputs of both the atomic and photonic subsystems. We investigate the behavior of the APIF function on the basis of three categories. The first case is that where the OFCS is much larger than the detuning parameter, is expressed as $\sqrt{2}v \gg \Delta_0$, while the opposite is for the second case, is expressed as $\Delta_0 \gg \sqrt{2}v$. The third case is that the OFCS is comparable to the augmented detuning, is expressed as $\sqrt{2}v \approx \Delta_0$. The investigation of the current model is limited to the case of starting the 1st-atom initially from its excited state while the 2nd-atom starts initially from its ground state. We numerically exhibit the cases of the appearance of the CRP whether the action of the ECFs is (through the augmented frequency) considered or not. Furthermore, we confine ourselves to handle the problem only with positive parameters.

5.1 Absence of the ECF

Now, we discuss the time evolution of the APIF due to changes in both the detuning and the strength of the optical fiber coupling in the numerical computations during the absence of the ECF is considered. The strategy is to enable one of the two control-

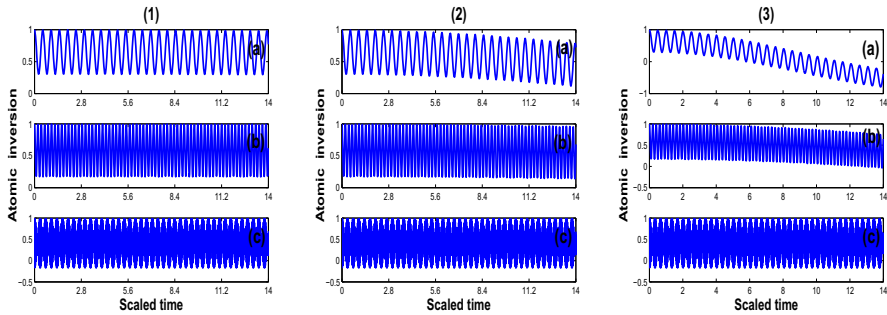


Fig. 5 Zoomed view of plots in Fig. 4

ling parameters (namely, the strength of the optical fiber coupling, and the localized detuning) to exceed the other.

5.1.1 Large OFCS and large detuning

Visualization of the role played by the addition of large value of the strength of the optical fiber coupling requires realizing the behavior of the APIF for two remote cavities *i.e.*, no an optical fiber mode and no a photon hopping. The figures and the numerical computations show that increasing the value of the localized detuning while the bosonic modes are uncorrelated shifts the minima of the atomic population inversion function upward and gives rise to more compressed Rabi-frequency (see frame(2a) in Fig. 2). This is an evidence that the rate of the quantum-information transfer between the atomic subsystems declines as a result of the increase of the value of the localized detuning. Generally speaking, the figures and the numerical computations indicate that the increase of the strength of the optical fiber coupling leads the APIF to exhibit periodic and regular oscillations of low frequency compared with those for the absence case and makes the APIF to reach almost its minimum extreme value in a periodic and a regular manner (compare frame(1a) with frame(a) in Fig. 2). The detuning parameter is of zero value (*i.e.*, $\Delta_0 = 0$), the contribution of the continuity of the increase of the strength of the optical fiber coupling adds nothing to the behavior of the APIF as long as the values of the OFCS overtake that for the atom-field coupling (see frame(1a) in Fig. 2). It is observed that the numerical computations showcase that the first atom spends longer time in its ground state compared with its excited state when both the detuning and the strength of the cavity-fiber coupling are not taken into account (see maxima and minima in frame(1a) in Fig. 2). The previous remark is a great motivation for addressing the case of having nonzero detuning. The pursuit to the controlling factor in the change of the rate of the quantum information transfer is principle reason behind this choice. The figures show that the reduction of the quantum-information transfer between the atomic subsystems is an inevitable result of the growth of the detuning in the numerical computations regardless of the absence and the presence of the optical fiber coupling although the associated features to its growing in the numerical computations are completely different with the two investigations (compare frame(1a) with frames(1b, 1c) in Fig. 2) and (compare among

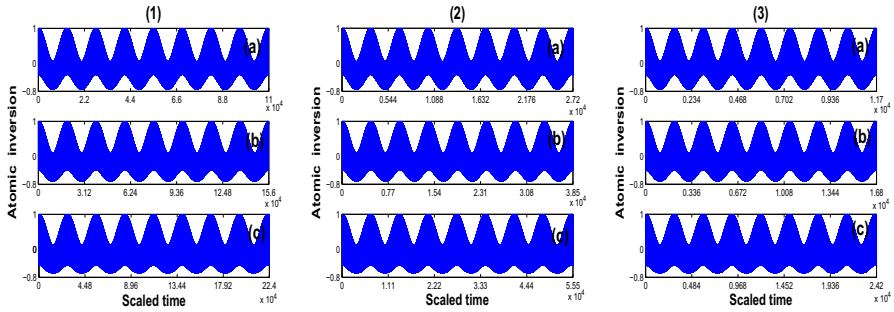


Fig. 6 The time evolution of the APIF of the 1^{st} -atom, $W_1(t)$, for the Hamiltonian Eq.(1) subject to the state Eq.(14) while the system parameters values are $\omega_0 = \Omega = 100\lambda$, and in (a) $\eta = \frac{1.350\pi}{9}$, (b) $\eta = \frac{1.400\pi}{9}$, and (c) $\eta = \frac{1.450\pi}{9}$, while in (1) $\sqrt{2}\nu = 5\lambda$, (2) $\sqrt{2}\nu = 10\lambda$, and in (3) $\sqrt{2}\nu = 15\lambda$

the different colored curves in frame(2) in Fig. 2). In detail, the factor $(\frac{1}{\Delta_1} + \frac{1}{\Delta_2} - \frac{2}{\Delta_0})$ controls the frequency of the APIF (see Fig. 2). Thus, one can manifest that the overlap between the values of both the detuning and the optical fiber coupling does not accord the same information (compare frame(1) with frame(2) in Fig. 2). All these results are in a complete conformity with those introduced in [96].

5.1.2 Comparable OFCS and detuning

Now, we draw the attention to the discussion of the behavior of the time evolution of the APIF when the difference between the localized detuning and the strength of the optical fiber coupling its magnitude is either zero (*i.e.*, the on resonance APIF, is depicted in frame(1) in Fig. 3) or infinitesimal value (*i.e.*, the near resonance APIF, is depicted in frames(2, 3) in Fig. 3). Their equal values (*i.e.*, Δ_0 , and $\sqrt{2}\nu$) are on the increase, interesting features are observed successively (*i*) modulating the amplitude until show what the so-called ring modulation (see frame(1) in Fig. 3), (*ii*) elongating the revivals periods (compare frame(1a) with frames(1b, 1c) in Fig. 3). When the detuning and the strength are of near resonance (*say*, $\Delta_0 \approx \sqrt{2}\nu$ with negative Δ_1), the resulted features are completely consistent with those for the on resonant case, except for nonequivalent quantum-information transfer between the atomic subsystems (compare frame(1) with frame(2) in Fig. 3). On the other hand, when $\Delta_0 \approx \sqrt{2}\nu$ with positive Δ_1 , the CRP is absent while the atomic population inversion function exhibits quasi-periodic oscillations (compare frame(1) with frame(3) in Fig. 3). The assertion nonexhibiting the APIF a CRP with positive near resonance Δ_1 , is not even remotely true, but it (*i.e.*, the CRP) can be appeared with much larger values of the detuning compared with those in on resonance and negative near resonance cases (plots are not considered here). Again, one can assert that the behavior of the APIF and the rate of the quantum-information transfer between the atomic subsystems may be controlled by the difference of the detuning and the strength of the optical fiber coupling (see Fig. 3). In other words, when the localized detuning and the strength of the optical fiber mode are approximately equal, the quantum-information transfer and the associated features are completely dependent on the change of Δ_1 . These three

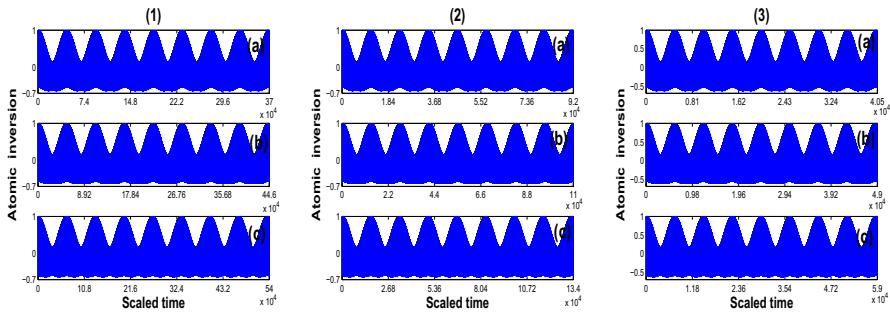


Fig. 7 The time evolution of the APIF of the 1^{st} -atom, $W_1(t)$, for the Hamiltonian Eq.(1) subject to the state Eq.(14) while the system parameters values are $\omega_0 = \Omega = 100\lambda$, and in (a) $\eta = \frac{1.520\pi}{9}$, (b) $\eta = \frac{1.545\pi}{9}$, and (c) $\eta = \frac{1.570\pi}{9}$, while in (1) $\sqrt{2}\nu = 5\lambda$, (2) $\sqrt{2}\nu = 10\lambda$, and in (3) $\sqrt{2}\nu = 15\lambda$

scenarios are in complete conformity with those appeared when the coupling between the cavities was by the overlap of evanescent cavity fields [98, 103].

5.2 Presence of the ECF

In this subsection, we are moving on towards addressing the effects of the ECFs on the time evolution of the APIF with giving essential differences between the current evolutions and their counterparts for the absence of the external classical fields was considered before. More clarification and fruitful investigation can be made through a harmonization among the controlling and relevant parameters. The investigation will be limited to the previously cited three investigated cases but with specific differences, given the augmentation of the localized due due to including the actions of the external classical fields.

5.2.1 Large OFCS and large detuning

– Large Delocalized Detuning

First of all, it is foreknown from the analytical results that the parameter η maps the relation between the atomic frequency and the coupling of the ECFs. Also, for a comprehensive investigation, we address two interesting categories, the first is exceeding the localized atomic frequencies to the couplings of the ECFs while the opposite is valid for the second category.

When $\eta \ll \frac{1}{2} \arctan \frac{4}{3}$, the figures and the numerical computations show that the increase of the ECF coupling not only leads the APIF to exhibit rapid and small oscillations "superpositions of fast and slow oscillations", but also, tends to the low frequency APIF and shift the minima of the APIF upward (compare frames(1a, 2a, 3a) with frames(1b-1c, 2b-2c, 3b-3c) respectively in Fig. 4). It is noticed that the action of the increase in the optical fiber coupling is immutable, its increase leads to shortening the revivals time (compare frame(1) with frames(2, 3) in Fig. 4). One can emphasize that the increase of the ECF coupling hinders the atom to populate its ground state (see Fig. 4). The aforementioned result is a direct

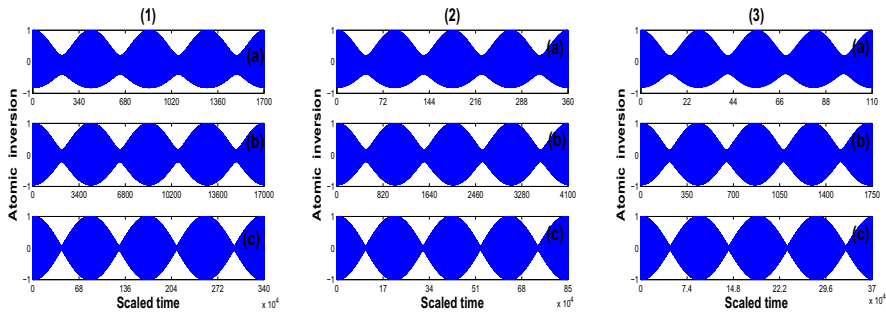


Fig. 8 The time evolution of the APIF of the 1^{st} -atom, $W_1(t)$, for the Hamiltonian Eq.(1) subject to the state Eq.(14) while the system parameters values are $\omega_0 = \Omega = 10\lambda$, and in (a) $\eta = \frac{1.800\pi}{9}$, (b) $\eta = \frac{2.000\pi}{9}$, and (c) $\eta = \frac{2.200\pi}{9}$, while in (1) $\sqrt{2}\nu = 5\lambda$, (2) $\sqrt{2}\nu = 10\lambda$, and in (3) $\sqrt{2}\nu = 15\lambda$

indication that the increase of the coupling of the ECFs hinders the effectiveness of the strength of the optical fiber coupling (compare Figs. 3 and 4 with Fig. 4). Finally, growth of the ECFC due to the variation of η with $\eta < < \frac{1}{2} \arctan \frac{4}{3}$ reduces in the quantum-information transfer rate between the atomic subsystems. Before proceeding to further investigations, we should clarify what in Fig. 4, they are the oscillations of the envelope of the revivals which carry fast oscillations (see Fig. 5). Moreover, we intend to deal with another two intervals, $\frac{1}{2} \arctan \frac{4}{3} < \eta < < \frac{\pi}{3}$, exhibited in Fig. 6, and $\frac{\pi}{3} < \eta < < \frac{1}{2} \arctan 2$, depicted in Fig. 7. One can easily observe that the action of the ECF coupling is somewhat similar to its counterpart when the values $\eta > > \frac{1}{2} \arctan 2$ were considered (compare Fig. 4 with Figs. 6 and 7).

The action of the increment of the ECF coupling not only it has the ability to lower the frequency of the APIF, but also, continuity of its increment leads to bringing the minima of the APIF upward (compare frames(1a, 2a, 3a) with frames(1b-1c, 2b-2c, 3b-3c) respectively in Figs. 4, 6 and 7). Being the atom is much far from its ground state is one of what differentiates the second interval from its predecessor (compare Fig. 4 with Figs. 6 and 7). Furthermore, beginning with $\eta > > \frac{1}{2} \arctan 2$, the time evolution of the APIF shows the expected phenomenon, namely; the CRP. Moreover, increasing the ECF coupling delays the appearance of the revivals periods and brings the minima of the APIF downward *i.e.*, increasing the coupling of the ECF is considered as an accelerator to the atom to reach its ground state (see Fig. 8). On the other hand, the sustained growth to the strength of the optical fiber coupling leads to shortening the revivals times (compare frame(1) with frames(2, 3) in Fig. 8). This observation is not for a specific interval but for all considered intervals (compare frame(1) with frames(2, 3) in Figs. 4, 6, 7 and 8).

Finally, it is obvious from the figures and the numerical computations that the rate of the elongation of the revivals times occurs as a result of the increase of the coupling of the ECFs and it is independent of the growth of the OFCS (compare frames(1a, 2a, 3a) with frames(1b-1c, 2b-2c, 3b-3c) respectively in Figs. 4, 6, 7 and 8). On the other hand, the rate of the shrinkage of the revivals times occurs

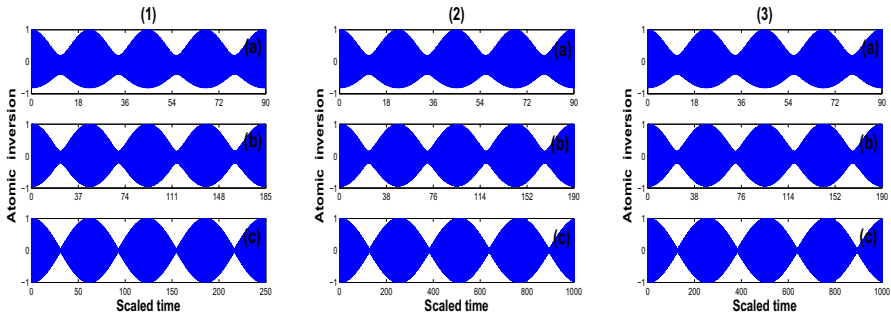


Fig. 9 The time evolution of the APIF of the 1^{st} -atom, $W_1(t)$, for the Hamiltonian Eq.(1) subject to the state Eq.(14) while the system parameters values are $\omega_0 = \Omega = 10\lambda$, and in (a) $\eta = \frac{1,800\pi}{9}$, (b) $\eta = \frac{2,000\pi}{9}$, and (c) $\eta = \frac{2,200\pi}{9}$, while in (1) $\sqrt{2}\nu = 250\lambda$, (2) $\sqrt{2}\nu = 500\lambda$, and (3) $\sqrt{2}\nu = 1000\lambda$.

as a result of the growth of the OFCS and it is independent of the ECFs coupling (compare frame(1) with frames(2, 3) in Figs. 4, 6, 7 and 8).

– Large OFCS

Generally speaking, when OFCS takes values far beyond its competitor (*i.e.*, the delocalized detuning), the features occur as a result of the growth of the ECFs in perfect match to those in the previous case (see Fig. 9). On the other hand, the role played by the continuity of the increase of the strength of the optical fiber coupling results in elongating the revivals periods. In fact, as in the case of the absence of the ECF, the strength of the optical fiber coupling adds no contribution when its value is much larger than that for the detuning (compare frame(1) with frames(2, 3) in Fig. 9).

5.2.2 Comparable OFCS and detuning

To go a step further, we pay some attention to investigate the considered scheme when the values of both the OFCS and augmented detuning are close to each others. Thus, this investigation must be compatible with the previously cited two hypotheses. The intelligibility of the present scenario may interrogate to stabilize the localized atomic frequency (*say*, $\Omega = 10\lambda$). Previously, we have mentioned that the argument η maps the relation between the augmented detuning and the atomic frequency. Based on the restrictions imposed in the current subsection, the strength of the optical fiber coupling becomes one of the relevant and controlling parameters. Considering a small value of the rotation angle η leads the APIF to show a chaotic behavior and the atom to become nearer to its ground state than its excited state. Increasing η not only gives rise to a shift upward of the mean of the APIF, but also causes an amplitude modulation. Such an amplitude modulation continues until the APIF exhibits the CRP. These collapses and revivals periods are greatly affected by the direct increase in the value of the argument (η) The revivals periods are prolonged as a result of the continuity of the increase of the rotation angle η . Finally, one can observe from the figures and the numerical computations that the atom does not have the ability to reach its destinations

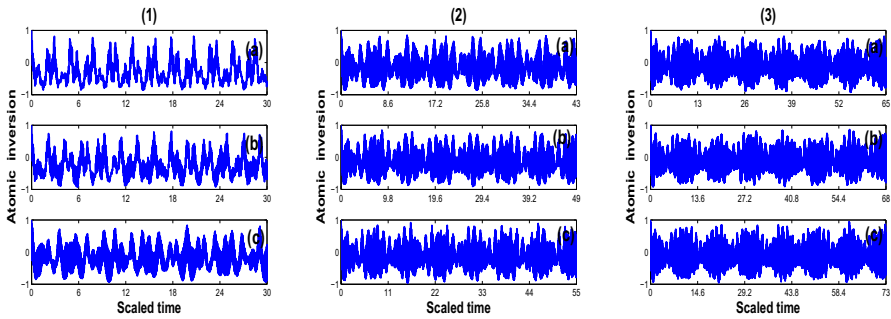


Fig. 10 The time evolution of the APIF of the 1^{st} -atom, $W_1(t)$, for the Hamiltonian Eq.(1) subject to the state Eq.(14) while the system parameters values are $\omega_0 = \Omega = 10\lambda$, and $\sqrt{2}\nu = \Delta_0$, while in (1), (a) $\eta = \frac{0.900\pi}{9}$, (b) $\eta = \frac{1.000\pi}{9}$, and (c) $\eta = \frac{1.250\pi}{9}$, in (2), (a) $\eta = \frac{1.350\pi}{9}$, (b) $\eta = \frac{1.400\pi}{9}$, and (c) $\eta = \frac{1.450\pi}{9}$ and in (3), (a) $\eta = \frac{1.520\pi}{9}$, (b) $\eta = \frac{1.545\pi}{9}$, and (c) $\eta = \frac{1.570\pi}{9}$

(compare frames(1a, 2a, 3a) with frames(1b-1c, 2b-2c, 3b-3c) respectively in Fig. 10). Ultimately, clearer collapses periods do not exist here. This may be attributed to having the vacuum states as initial states of the fields and no photons distributions are involved.

5.3 The second atom information

As we have mentioned before, the purpose of the current work is to track the behavior of the QST and to indicate the essential difference between the rates of the transfer in the two schemes: The current scheme and the scheme in [97]. First, we intend to introduce some differences between the time evolutions of the APIFs, $W_1(t)$, and $W_2(t)$ in the numerical computations point of view. Second, through corresponding inputs in the two schemes and the effective Hamiltonians, we review and state which of the two schemes is of higher transfer rate?. It is preferable to address the numerical computations in the framework of the large OFCS limit seeing its intelligibility. The addressability will not only for the absence of the action of the ECFCs but also will be for the case of its presence. Based on the numerical computations and Figs. 2, 3 and Figs. 11, 12) one can approve what we have mentioned before: Perfect atomic states transfer is possible when $\sum_{i=1}^2 W_i(t) = 0$, while synchronization of the two atoms is also possible when $\sum_{i=1}^2 (-)^{i+1} W_i(t) = 0$. No need to call the corresponding figure of the other scheme to give an essential difference, enough to state that the rate of the energy transfer with the current scheme is higher compared with that for the other scheme. Moreover, it is observable when no action for the ECFCs, there is no a transfer for the energy between the atomic subsystems as long as there no a transmission line (compare frame(2a) in Fig. 2 with frame(2a) in Fig. 11). It is worth noting, when no a photons can be transfer from a cavity to another while the action of the ECFCs is considered, there is a possibility for the energy transferred between the atomic subsystems (plots are not shown here).

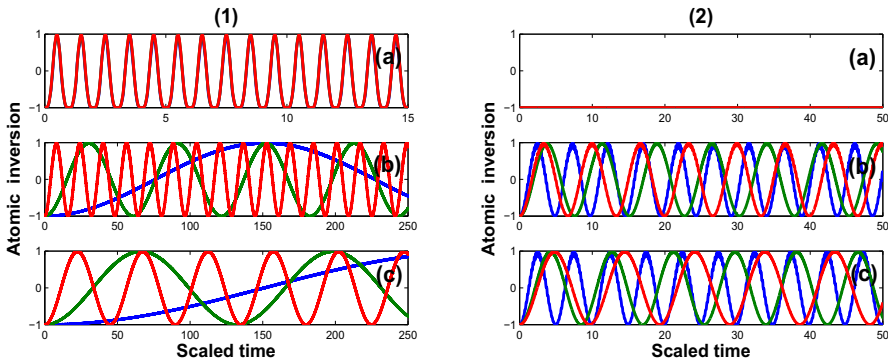


Fig. 11 The time evolution of the AIPF of the 2^{nd} -atom, $W_2(t)$, for the Hamiltonian Eq.(1) with the same parameters of the system which are exploited in the numerical computations for the Fig.(2)

6 Conclusion

In the aforementioned, we have investigated the CRP in the context of the AIPF due to the influences of the atomic frequencies, localized and delocalized detuning, the couplings of the ECFs, and the OFCS. The investigation has been carried out based on the condition that the atom-field coupling is small comparable with the other parameters. The investigation has been analytically and numerically presented in the context of three dispersive regimes approximations as stated in the text. The general conclusions reached and illustrated by numerical results show that:

- The AIPF is of a sinusoidal behavior as long as the action of the ECF is not considered while both the detuning and the OFCS have big differences in this case low increasing of the OFCS causes swinging the atom between its upper and lower states through the time evolution of the AIPF".
- Prolongation and shrinkage of the revivals periods are controlled by the difference between both the detuning and the OFCS or rather controlled by the factor $(\frac{1}{\Delta_1} + \frac{1}{\Delta_2} - \frac{2}{\Delta_0})$. Compressing and broadening the frequencies of the fluctuations of the AIPF are also dependent on this difference or rather controlled by the same factor $(\frac{1}{\Delta_1} + \frac{1}{\Delta_2} - \frac{2}{\Delta_0})$.
- The actions of the ECFs are not considered, the AIPF exhibits a CRP provided the detuning and the OFCS are having nonzero values but either on resonance or near resonance.
- The actions of the couplings of the ECFs are of wider range. This is attributed to the fact that they are not only confined to the inclusion of the augmented detuning but also extend to the determination of their place values to those of atomic frequencies.
- In consideration of the above-mentioned case, the minima of the AIPF go downward as a result of the continuous increase of the couplings the external fields and their exceeding to a specific value of the localized atomic frequency.
- In contrast, the minima of the AIPF go upward as a result of the continuous increase of the couplings ECFs: monotonically, (i) exceeding the delocalized detuning to

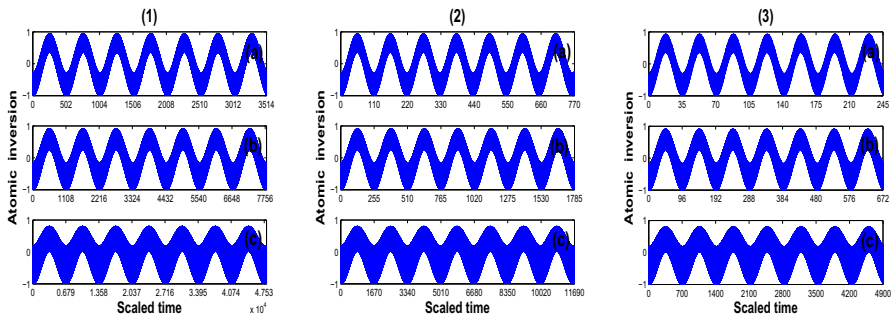


Fig. 12 The time evolution of the APIF of the 2^{nd} -atom, $W_2(t)$, for the Hamiltonian Eq.(1) with the same parameters of the system which are exploited in the numerical computations for Fig. 3

the localized atomic frequency (*ii*) exceeding the localized atomic frequency to both the delocalized detuning and the ECF coupling respectively (*iii*) exceeding the localized atomic frequency to both the ECF coupling and the delocalized detuning.

- The APIF exhibits the CRP when the couplings of the ECFs exceed the localized atomic frequency whether the OFCS exceeds the augmented detuning or not.
- When the augmented detuning is on resonance or near resonance to the OFCS, incomplete CRP rises compared with its counterparts whether in the presence of the ECFs or not.
- The dispersive regimes are ones of the controlling factors for the rate of the energy transfer between the atomic subsystems: Each one of them is associated to a specific rate; no one of them is commensurate to the other.

Acknowledgements Authors thank Taif University Researchers Supporting Project number (TURSP-2020/17), Taif University, Taif, Saudi Arabia.

References

1. Jaynes, E.T., Cummings, F.W.: Comparison of quantum and semiclassical radiation theories with application to the beam maser. *Proc. IEEE* **51**, 89 (1963)
2. Eberly, J.H., Narozhny, N.B., Sanchez-Mondragan, J.J.: Periodic spontaneous collapse and revival in a simple quantum model. *Phys. Rev. Lett.* **44**, 1323 (1980)
3. Eberly, J.H., Narozhny, N.B., Sanchez-Mondragan, J.J.: Coherence versus incoherence: Collapse and revival in a simple quantum model. *Phys. Rev. A.* **23**, 236 (1981)
4. Rempe, C., Walther, H., Klein, N.: Observation of quantum collapse and revival in a one-atom maser. *Phys. Rev. Lett.* **58**, 353 (1987)
5. Walther, H.: The Single Atom Maser and the Quantum Electrodynamics in a Cavity. *Phys. Scr.* **T23**, 165 (1988)
6. Eberly, J.H., Narozhny, N.B., Sanchez-Mondragan, J.J.: Theory of Spontaneous-Emission Line Shape in an Ideal Cavity. *Phys. Rev. Lett.* **51**, 550 (1983)
7. Agarwal, G.S.: Vacuum-field Rabi oscillations of atoms in a cavity. *J. Opt. Soc. Am. B* **2**, 480 (1983)
8. Agarwal, G.S.: Vacuum-Field Rabi Splittings in Microwave Absorption by Rydberg Atoms in a Cavity. *Phys. Rev. Lett.* **53**, 1732 (1984)
9. Stenholm, S.: Quantum theory of RF resonances: the semiclassical limit. *Phys. Rep.* **6C**, 1 (1973)

10. Stenholm, S.: A Bargmann representation solution of the Jaynes-Cummings model. *Opt. Commun.* **36**, 75 (1981)
11. Von Foerster, T.: A comparison of quantum and semi-classical theories of the interaction between a two-level atom and the radiation field. *J. Phys. A* **8**, 95 (1975)
12. Meystre, P., Geneax, E., Quattropiani, A., Faish, F.: Long-time behaviour of a two-level system in interaction with an electromagnetic field. *Nuovo Cimento B* **25**, 521 (1975)
13. Eberly, J.H., Narozhny, N.B., Sanchez-Mondragon, J.J.: Four-momentum transfer between groups of secondary particles in proton-nucleus interactions at 200 GeV. *Phys. Rev. A* **23**, 14 (1981)
14. Yoo, H.-I., Eberly, J.H.: Dynamical theory of an atom with two or three levels interacting with quantized cavity fields. *Physics Reports* **118**, 239 (1985)
15. Knight, P.L., Milonni, P.W.: The Rabi frequency in optical spectra. *Phys. Rep* **66c**, 21 (1980)
16. Knight, P.L., Radmore, P.M.: Quantum revivals of a two-level system driven by chaotic radiation. *Phys. Lett.* **90A**, 342 (1982)
17. Knight, P.L.: Quantum Fluctuations and Squeezing in the Interaction of an Atom with a Single Field Mode. *Phys. Scr.* **T12**, 51 (1986)
18. Meystre, P., Zubairy, M.S.: Squeezed states in the Jaynes-Cummings model. *Phys. Lett.* **89A**, 390 (1982)
19. Singh, S.: Field statistics in some generalized Jaynes-Cummings models. *Phys. Rev. A* **25**, 3206 (1982)
20. Milburn, G.J.: Interaction of a Two-level Atom with Squeezed Light. *Opt. Acta* **31**, 671 (1984)
21. Barnett, S.M., Filipowicz, F., Javanainen, J., Knight, P.L., Meystre, P.: The Jaynes-cummings model and beyond. *Frontiers Quantum Opt.* **31**, 485–520 (1984)
22. Compagno, G., Peng, J.S., Persico, F.: Squeezing in a two-photon Dicke hamiltonian. *Opt. Commun.* **57**, 415 (1986)
23. Carmichael, H.J.: Photon Antibunching and Squeezing for a Single Atom in a Resonant Cavity. *Phys. Rev. Lett.* **55**, 2790 (1985)
24. Pui, R.R., Agarwal, G.S.: Collapse and revival phenomena in the Jaynes-Cummings model with cavity damping. *Phys. Rev. A* **33**, 3610 (1986)
25. Kuklinski, J.R., Madajczyk, J.L.: Strong squeezing in the Jaynes-Cummings model. *Phys. Rev. A* **37**, 3175 (1988)
26. Dick, R.H.: Coherence in spontaneous radiation processes. *Phys. Rev.* **93**, 99 (1954)
27. Tavis, M., Cummings, F.W.: Exact Solution for an N -Molecule-Radiation-Field Hamiltonian. *Phys. Rev.* **170**, 379 (1968)
28. Abdalla, M.S., Ahamed, M.M., Obada, A.-S.F.: Dynamics of a non-linear Jaynes-Cummings model. *Phys. A* **162**, 215 (1990)
29. Abdalla, M.S., Ahmed, M.M., Obada, A.-S.F.: Multimode and multiphoton processes in a non-linear Jaynes-Cummings model. *Phys. A* **170**, 393 (1991)
30. Abdalla, M.S., Abdel-Aty, M., Obada, A.-S.F.: Quantum entropy of isotropic coupled oscillators interacting with a single atom. *Opt. Commun.* **211**, 225 (2002)
31. Abdalla, M.S., Abdel-Aty, M., Obada, A.-S.F.: Degree of entanglement for anisotropic coupled oscillators interacting with a single atom. *J. Opt. B: Quantum Semiclass. Opt.* **4**, 396 (2002)
32. Marchiolli, M.A., Missori, R.J., Roversi, J.A.: Qualitative aspects of entanglement in the Jaynes-Cummings model with an external quantum field. *J. Phys. A* **36**, 12275 (2003)
33. Obada, A.-S.F., Abdalla, M.S., Khalil, E.M.: Statistical properties of two-mode parametric amplifier interacting with a single atom. *Physica A* **336**, 433 (2004)
34. Obada, A.-S.F., Hanoura, S.A., Eied, A.A.: Entanglement of a multi-photon three-level atom interacting with a single-mode field in the presence of nonlinearities. *Eur. Phys. J. D* **66**, 221 (2012)
35. Obada, A.-S.F., Hanoura, S.A., Eied, A.A.: Quantum Entropy of a Four-Level Atom with Arbitrary Nonlinearities. *Int. J. Theor. Phys.* **51**, 2665 (2012)
36. Obada, A.-S.F., Hanoura, S.A., Eied, A.A.: Entropy of a general three-level atom interacting with a two mode. *Laser Phys.* **23**, 025201 (2013)
37. Obada, A.-S.F., Hanoura, S.A., Eied, A.A.: Entanglement for a general formalism of a three-level atom in a V-configuration interacting nonlinearly with a non-correlated two-mode field. *Laser Phys.* **23**, 055201 (2013)
38. Obada, A.-S.F., Hanoura, S.A., Eied, A.A.: Collapse-revival phenomenon for different configurations of a three-level atom interacting with a field via multi-photon process and nonlinearities. *Eur. Phys. J. D* **68**, 18 (2014)

39. Obada, A.-S.F., Hanoura, S.A., Eied, A.A.: Entanglement for a general formalism of a three-level atom in an Ξ -configuration interacting nonlinearly with a non-correlated two-mode field. *Optik* **136**, 602 (2017)
40. Obada, A.-S.F., Hanoura, S.A., Eied, A.A.: Entanglement in a system of a three-level atom interacting with a single-mode field in the presence of arbitrary forms of the nonlinearity and of the atomic initial state. *Laser Phys.* **24**, 055201 (2014)
41. Makhviladze, T.M., Shelepin, L.A.: Cooperative effects in radiation processes (multilevel particles and second-order perturbation theory). *Phys. Rev. A* **9**, 538 (1974)
42. Bogolubov, N.N., Jr., Le Kien, F., Shumovski, A.S.: Two-phonon process in a three-level system. *Phys. Lett. A* **101**, 201 (1984)
43. Abdel-Hafez, A.M., Ahamed, M.M., Obada, A.-S.F.: N-level atom and N-1 modes: Statistical aspects and interaction with squeezed light. *Phys. Rev. A* **34**, 1634 (1987)
44. Obada, A.-S.F., Eied, A.A.: Entanglement in a system of an Ξ -type three-level atom interacting with a non-correlated two-mode cavity field in the presence of nonlinearities. *Opt. Commun.* **282**, 2184 (2009)
45. El-Deberky, M.A.A.: The dynamical effect of stark-shifts produced from a four-level atomic system. *Int. J. Phys. Sci.* **4**, 253 (2009)
46. Abdel-Wahab, N.H.: A moving four-level N-type atom interacting with cavity fields. *J. Phys. B: At. Mol. Opt. Phys.* **41**, 105502 (2008)
47. Tavis, M., Cummings, F.W.: Exact Solution for an Ξ -Molecule-Radiation-Field Hamiltonian. *Phys. Rev* **170**, 379 (1968)
48. Brune, M., Schmidt-Kaler, F., Maali, A., Dreyer, J., Raimond, J.M., Haroche, S.: Exact Solution for an Ξ -Molecule-Radiation-Field Hamiltonian. *Phys. Rev. Lett.* **76**, 1800 (1996)
49. Rempe, G., Walter, H., Klein, N.: Microlaser: A laser with one atom in an optical resonator. *Phys. Rev. Lett.* **58**, 353 (2000)
50. Schmidt-Kaler, F., Maali, A., Dreyer, J., Haglet, E., Raimond, J.M., Haroche, S.: Observing the progressive decoherence of the "meter" in a quantum measurement. *Phys. Rev. Lett.* **76**, 1800 (1996)
51. Schlicher, R.R.: Jaynes-Cummings model with atomic motion. *Opt. Commun.* **70**, 97 (1989)
52. Gea-Banacloche, J.: Collapse and revival of the state vector in the Jaynes-Cummings model: An example of state preparation by a quantum apparatus. *Phys. Rev. Lett.* **65**, 3385 (1990)
53. Goldberg, P., Harrison, L.C.: Electric field in the coherent-state Jaynes-Cummings model. *Phys. Rev. A* **43**, 376 (1991)
54. Satyanarayana, M.V., Vijayakumar, M., Asling, P.: Glauber-Lachs version of the Jaynes-Cummings interaction of a two-level atom. *Phys. Rev. A* **45**, 5301 (1992)
55. Shore, B.W., Knight, P.L.: The jaynes-cummings model. *J. Mod. Opt.* **40**, 1195 (1993)
56. Vernooy, D.W., Kimble, J.H.: Well-dressed states for wave-packet dynamics in cavity QED. *Phys. Rev. A* **56**, 4287 (1997)
57. Zou, X.-B., Xu, J.-B.: Interaction of a two-level atom with a quantized radiation field in the presence of a gravitational field. *Phys. Rev. A* **61**, 063409 (2000)
58. Doherty, A.C., Lynn, T.W., Hood, C.J., Kimble, H.J.: Trapping of single atoms with single photons in cavity QED. *Phys. Rev. A* **63**, 013401 (2000)
59. Eberly, J.H., Narozhny, N.B., Sanchez-Mondragon, J.J.: Oscillations, decay, and recurrences in a simple quantum model. *Sov. J. Quantum Electron* **10**, 1261 (1981)
60. Buek, B., Sukumar, C.V.: Exactly soluble model of atom-phonon coupling showing periodic decay and revival. *Phys. Lett.* **81A**, 132 (1981)
61. Sukumar, C.V., Buek, B.: Multi-phonon generalisation of the Jaynes-Cummings model. *Phys. Lett.* **83A**, 211 (1981)
62. Cirac, J.I., Ekert, A.K., Huelga, S.F., Macchiavello, C.: Distributed quantum computation over noisy channels. *Phys. Rev. A* **59**, 4249 (1999)
63. Bennett, C.H., Brassard, G., Popescu, S., Schumacher, B., Smolin, J.A., Wootters, W.K.: Mixed-state entanglement and quantum error correction. *Phys. Rev. Lett.* **76**, 722 (1996)
64. Jennewein, T., Simon, C., Weihs, G., Weinfurter, H., Zeilinger, A.: Quantum cryptography with entangled photons. *Phys. Rev. Lett.* **84**, 4729 (2000)
65. You, J.Q., Tsai, J.S., Nori, F.: Scalable quantum computing with Josephson charge qubits. *Phys. Rev. Lett.* **89**, 197902 (2002)
66. Peřina, J., Haderka, O., Soubusta, J.: Quantum cryptography using a photon source based on postselection from entangled two-photon states. *Phys. Rev. A* **64**, 052305 (2001)

67. Recati, A., Calarco, T., Zanardi, P., Cirac, J.I., Zoller, P.: Holonomic quantum computation with neutral atoms. *Phys. Rev. A* **66**, 032309 (2002)
68. Li, G.-X., Tan, H., Macovei, M.: Enhancement of entanglement for two-mode fields generated from four-wave mixing with the help of the auxiliary atomic transition. *Phys. Rev. A* **76**, 053827 (2004)
69. Li, G.-X., Ke, S., Ficek, Z.: Generation of pure continuous-variable entangled cluster states of four separate atomic ensembles in a ring cavity. *Phys. Rev. A* **79**, 033827 (2009)
70. Hu, X.M., Zou, J.H.: Quantum-beat lasers as bright sources of entangled sub-Poissonian light. *Phys. Rev. A* **78**, 045801 (2008)
71. Li, X., Hu, X.M.: Tripartite entanglement in quantum-beat lasers. *Phys. Rev. A* **80**, 023815 (2009)
72. Deutsch, D., Ekert, A., Jozsa, R., Macchiavello, C., Popescu, S., Sanpera, A.: Quantum privacy amplification and the security of quantum cryptography over noisy channels. *Phys. Rev. Lett.* **77**, 2818 (1996)
73. Deng, Z.J., Feng, M., Gao, K.L.: Preparation of entangled states of four remote atomic qubits in decoherence-free subspace. *Phys. Rev. Lett.* **75**, 024302 (2007)
74. Fischer, D.G., Mack, H., Freyberger, M.: Transfer of quantum states using finite resources. *Phys. Rev. A* **63**, 042305 (2001)
75. Yönaç, Muhammed, Eberly, J.H.: Coherent-state control of noninteracting quantum entanglement. *Phys. Rev. A* **82**, 022321 (2010)
76. Yönaç, Muhammed, Eberly, Joseph H.: Qubit entanglement driven by remote optical fields. *Opt. Lett.* **33**, 270 (2008)
77. Blanco, P., Mundarain, D.: Faithful entanglement transference from qubits to continuous variable systems. *J. Phys. B: At. Mol. Opt. Phys.* **44**, 105501 (2011)
78. Yao-Hua, Hu., Jun-Qiang, Wang: Quantum correlations between two non-interacting atoms under the influence of a thermal environment. *Chin. Phys. B* **21**, 014203 (2012)
79. Son, W., Kim, M.S., Lee, Jinyoung, Ahn, D.: Entanglement transfer from continuous variables to qubits. *J. Mod. Opt.* **49**, 1739 (2002)
80. Zou, Hong-Mei., Fang, Mao-Fa.: Analytical solution and entanglement swapping of a double Jaynes-Cummings model in non-Markovian environments. *Quantum Inf. Proc.* **14**, 2673 (2015)
81. Chen, Qing-Hu., Yang, Yuan, Liu, Tao, Wang, Ke-Lin.: Entanglement dynamics of two independent Jaynes-Cummings atoms without the rotating-wave approximation. *Phys. Rev. A* **82**, 052306 (2010)
82. Chan, Stanley, Reid, M.D., Ficek, Z.: Entanglement evolution of two remote and non-identical Jaynes-Cummings atoms. *J. Phys. B: At. Mol. Opt. Phys.* **42**, 065507 (2009)
83. Sainz, Isabel, Björk, Gunnar: Entanglement invariant for the double Jaynes-Cummings model. *Phys. Rev. A* **76**, 042313, 052305 (2007)
84. Lee, Jinyoung, Paternoistro, M., Kim, M.S., Bose, S.: Entanglement reciprocation between qubits and continuous variables. *Phys. Rev. Lett.* **96**, 080501 (2006)
85. Yönaç, Muhammed, Eberly, Joseph H.: Sudden death of entanglement of two Jaynes-Cummings atoms. *J. Phys. B: At. Mol. Opt. Phys.* **39**, S621 (2006)
86. Cao, Bao-Liang., Shi, Ying, Jiang, Dong-Guang.: The dynamics of quantum correlations between two atoms in two coupled cavities. *Int. J. Theor. Phys.* **53**, 1920 (2014)
87. Bougouffa, Smail, Ficek, Zbignew: Atoms versus photons as carriers of quantum states. *Phys. Rev. A* **88**, 022317 (2013)
88. Trieu, Duong Hai: Dynamics in a system of four qubits in two cavities. *J. Phys.: Conf. Ser.* **187**, 012032 (2009)
89. Zhang, Ke., Li, Zhi-Yuan.: Transfer behavior of quantum states between atoms in photonic crystal coupled cavities. *Phys. Rev. A* **81**, 033843 (2010)
90. Enríquez, Marco, Quintana, Claudia, Rosas-Ortiz, Oscar: Time-evolution of entangled bipartite atomic systems in quantized radiation fields. *J. Phys.: Conf. Ser.* **512**, 012022 (2014)
91. Hanoura, S.A., Ahmed, M.M.A., Khalil, E.M., Obada, A.-S.F.: Single-Atom Entanglement for a System of Directly Linked Two Cavities in the Presence of an External Classical Field: Effect of Atomic Coherence. *Fortschr. Phys.* **67**, 1800101 (2019)
92. Hanoura, S.A., Ahmed, M.M.A., Khalil, E.M., Obada, A.-S.F.: Entanglement dynamics of a dispersive system of two driven qubits localized in coherently two linked optical cavities: two dispersive spatial distant driven Jaynes -Cummings cells. *Opt Quant Electron* **54**, 11 (2022). <https://doi.org/10.1007/s11082-021-02964-2>

93. Hanoura, S.A., Ahmed, M.M.A., Khalil, E.M., Obada, A.-S.F.: Quantum entropy of a two-linked Jaynes-Cummings cells for single-excitation quantum states. *Modern Physics Letters*. **34**, 1950093 (2019)
94. Lü, Xin-You., Si, Liu-Gang., Wang, Meng, Zhang, Su-Zhen., Yang, Xiaoxue: Generation of entanglement between two spatially separated atoms via dispersive atom-field interaction. *J. Phys. B: At. Mol. Opt. Phys.* **41**, 235502 (2008)
95. Nohama, F.K., Roversi, J.A.: Two-qubit state transfer between trapped ions using electromagnetic cavities coupled by an optical fibre. *J. Phys. B: At. Mol. Opt. Phys.* **41**, 045503 (2008)
96. Liao, Chang-Geng., Yang, Zhen-Biao., Luo, Cheng-Li., Chen, Zi-Hong.: Dynamics for two cavity QED systems coupled by an optical fiber. *Opt. Commun.* **284**, 1920 (2011)
97. Hanoura, S.A., Ahmed, M.M.A., Khalil, E.M., Obada, A.-S.F.: Collapses-revivals phenomenon of a system of a two-linked cavities in the presence of an external classical field. *Phys. E Low Dimens. Syst. Nanostruct.* **117**, 113163 (2020)
98. Ogden, C.D., Irish, E.K., Kim, M.S.: Dynamics in a coupled-cavity array. *Phys. Rev. A* **78**, 063805 (2008)
99. Khalil, E.M.: Influence of the external classical field on the entanglement of a two-level atom. *Int. J. Theor. Phys.* **52**, 1122 (2013)
100. Sebawe Abdalla, M., Obada, A.-S. F., Khalil, E. M., Ali, S. I.: The influence of phase damping on a two-level atom in the presence of the classical laser field. *Laser Phys.* **23**, 115201 (2013)
101. Sebawe Abdalla, M., Obada, A. S. F.: Exact treatment of the Jaynes-Cummings model under the action of an external classical field. *Ann. Phys.* **326**, 2486 (2011)
102. Shen, Li-Tuo., Yang, Zhen-Biao., Huai-Zhi, Wu., Chen, Xin-Yu., Zheng, Shi-Biao.: Control of two-atom entanglement with two thermal fields in coupled cavities. *J. Opt. Soc. Am. B* **29**, 2379 (2012)
103. Jun, Peng, Yun-Wen, Wu., Xiao-Juan, Li.: Quantum dynamic behaviour in a coupled cavities system. *Chin. Phys. B* **21**, 060302 (2012)
104. Louisell, W.H.: *Quantum statistical properties of radiation*. John Wiley, Sons Canada (1973)
105. James, D.F., Jerke, J.: Effective Hamiltonian theory and its applications in quantum information. Transfer behavior of quantum states between atoms in photonic crystal coupled cavities. *Can. J. Phys* **85**, 625 (2007)
106. Zhang, Ke., Li, Zhi-Yuan.: Transfer behavior of quantum states between atoms in photonic crystal coupled cavities. *Phys. Rev. A* **81**, 033843 (2010)
107. Scully, M.O., Zubairy, M.S.: *Quantum optics*. Cambridge University Press, Cambridge (1997)
108. Peřina, Jr., Peřina, J.: *Progress in optics*. Elsevier, Amsterdam (2000)

Publisher's Note Springer Nature remains neutral with regard to jurisdictional claims in published maps and institutional affiliations.